Crystal Structure and NQR Studies of Compounds (RH)[$ZnBr_3$(R)], $(RH)_2[ZnBr_4]$ and $[ZnBr_2(R)_2]$ (R = Py, *n*-MePy: *n* = 2, 3, 4); on the Dominant Stability of the Monoanionic Complexes over the Dianionic and Neutral Species

Hideta Ishihara[a], Michio Nakashima[a], Hisayo Nakashima[a], Ryuichi Tateno[a], Yuki Shibamura[a], Toshio Makino[a], Aika Kikuchi[a], Daisuke Kii[a], Keizo Horiuchi[b], Ingrid Svoboda[c], Hartmut Fuess[c], and Hiromitsu Terao[d]

[a] Faculty of Culture and Education, Saga University, Saga 840-8502, Japan
[b] Faculty of Science, University of the Ryukyus, 1 Senbaru, Okinawa 903-0213, Japan
[c] Materials Science, University of Technology, Petersenstraße 23, 64287 Darmstadt, Germany
[d] Faculty of Integrated Arts and Sciences, Tokushima University, Tokushima 770-8502, Japan

Reprint requests to Prof. H. Ishihara. E-mail: isiharah@cc.saga-u.ac.jp

Z. Naturforsch. **2011**, *66b,* 27 – 35; received August 27, 2010

The monoanionic complexes (C_5H_5NH)[$ZnBr_3(C_5H_5N)$] (**1**) and (*n*-$CH_3C_5H_4NH$)[$ZnBr_3$(*n*-$CH_3C_5H_4N$)] (*n* = 2 (**2**), 3 (**3**), 4 (**4**)) were prepared by crystallization from ethanol solutions through redistribution reactions between the corresponding dianionic complexes $(C_5H_5NH)_2[ZnBr_4]$ (**5**) and $(n\text{-}CH_3C_5H_4NH)_2[ZnBr_4]$ (*n* = 2, 3 (**6**), 4 (**7**)) and the neutral complexes $[ZnBr_2(C_5H_5N)_2]$ (**10**) and $[ZnBr_2(n\text{-}CH_3C_5H_4N)_2]$ (*n* = 2 (**8**), 3, 4 (**9**)). The crystal structures of **1**, **4**, **9**, and **10** were determined; **1**: triclinic, $P\bar{1}$, a = 7.6957(5), b = 7.7975(4), c = 12.4768(8) Å, α = 90.857(5), β = 95.917(5), γ = 107.899(6)°, Z = 2, 150 K; **4**: monoclinic, $P2_1/c$, a = 14.8369(6), b = 13.9504(5), c = 8.0041(3) Å, β = 96.318(4)°, Z = 4, 299 K; **9**: monoclinic, $P2_1/c$, a = 14.2883(5), b = 8.0269(3), c = 13.6031(5) Å, β = 100.581(4)°, Z = 4, 150 K; **10**: monoclinic, $P2_1/c$, a = 8.7388(5), b = 17.9730(10), c = 8.5452(5) Å, β = 100.024(6)°, Z = 4, 300 K. The cation and anion are paired up *via* bifurcated hydrogen bonds in the structure of **1** and *via* a normal N–H···Br hydrogen bond in the structure of **4**. ^{81}Br NQR resonance lines coinciding in number with the Br atoms in the chemical formulae were observed for the compounds **1** – **5** and **7** – **9** throughout the temperature range from 77 to *ca.* 320 K. The comparison between the net charges on the Br atoms obtained by the Townes-Daily analysis or by the Mulliken population analysis seems to indicate that the formation of the intermolecular N–H···Br hydrogen bonds and the π-π and the CH_3-π interactions in the crystal structures of the monoanionic complexes are the driving forces to the redistribution reactions.

Key words: Zinc(II) Bromide Complexes, ^{81}Br NQR, Crystal Structure, Intermolecular Interactions

Introduction

Three types of zinc bromide complexes with pyridines (R), *i. e.* $[ZnBr_2(R)_2]$, (RH)[$ZnBr_3$(R)], and $(RH)_2[ZnBr_4]$, constitute an interesting group, where the Zn atoms have tetrahedral coordination, and the charges on the complexes vary from 0 to −2 with increasing numbers of Br atoms. The monoanionic complexes (RH)[$ZnBr_3$(R)] tend to be formed in redistribution reactions from mixtures of the neutral $[ZnBr_2(R)_2]$ and the dianionic complexes $(RH)_2[ZnBr_4]$ in ethanol solutions. This tendency may indicate that the former are more stable compared to the combination of the other two types. In this work we have tried to prepare a series of the complex compounds of zinc bromide with pyridines, (RH)[$ZnBr_3$(R)], $(RH)_2[ZnBr_4]$ and $[ZnBr_2(R)_2]$ (R = Py, *n*-MePy: *n* = 2, 3, 4), to confirm the occurrence of the redistribution reactions and to investigate the relations of structures and electronic states among the related compounds.

Nuclear quadrupole resonance (NQR) spectroscopy is an experimental technique which is very useful to elucidate the electronic distributions around the relevant nuclei in crystalline solids, which has thus been intensively used in studying chemical bonding, crystal structures, phase transitions, *etc.* We have applied halogen NQR to investigate a series of the complex compounds of zinc and cadmium halides with alkyl

Table 1. Crystallographic data and experimental conditions for the crystal structure determinations of **1**, **4**, **9**, and **10**.

	1	**4**	**9**	**10**
Formula	$C_{10}H_{11}Br_3N_2Zn$	$C_{12}H_{15}Br_3N_2Zn$	$C_{12}H_{14}Br_2N_2Zn$	$C_{10}H_{10}Br_2N_2Zn$
M_r	464.30	492.36	411.14	383.39
Crystal size, mm^3	$0.24 \times 0.20 \times 0.12$	$0.50 \times 0.28 \times 0.12$	$0.50 \times 0.26 \times 0.20$	$0.40 \times 0.20 \times 0.16$
Crystal system	triclinic	monoclinic	monoclinic	monoclinic
Space group	$P\bar{1}$	$P2_1/c$	$P2_1/c$	$P2_1/c$
a, Å	7.6957(5)	14.8369(6)	14.2883(5)	8.7388(5)
b, Å	7.7975(4)	13.9504(5)	8.0269(3)	17.9730(10)
c, Å	12.4768(8)	8.0041(3)	13.6031(5)	8.5452(5)
α, deg	90.857(5)	90	90	90
β, deg	95.917(5)	96.318(4)	100.581(4)	100.021(6)
γ, deg	107.899(6)	90	90	90
Z	2	4	4	4
D_{calcd}, g cm^{-3}	2.18	1.99	1.78	1.78
Temperature, K	150(2)	299(2)	150(2)	300(2)
$\mu(MoK_\alpha)$, mm^{-1}	10.2	8.8	6.8	7.9
$F(000)$, e	440	944	800	736
θ range, deg	3.08 – 26.37	2.76 – 26.37	2.92 – 26.37	2.62 – 26.37
hkl range	$-9 \le h \le 9$, $-9 \le k \le 8$, $-15 \le l \le 13$	$-18 \le h \le 13$, $-17 \le k \le 17$, $-10 \le l \le 10$,	$-14 \le h \le 17$, $-10 \le k \le 7$, $-13 \le l \le 7$	$-10 \le h \le 10$, $-22 \le k \le 22$, $-10 \le l \le 10$
$((\sin.\theta)/.\lambda)_{max}$, $Å^{-1}$	0.6249	0.6249	0.6249	0.6249
Refl. measd. / unique / R_{int}	4751 / 2874 / 0.0196	11649 / 3352 / 0.0278	6360 / 3132 / 0.0158	9334 / 2698 / 0.0265
Refl. with $[I \ge 2\sigma(I)]$	2039	2465	2559	1850
Param. refined	148	169	154	136
$R(F)/wR(F^2)$[a] $[I \ge 2\sigma(I)]$	0.0283 / 0.0566	0.0351 / 0.0802	0.0242 / 0.0585	0.0275 / 0.0625
GoF(F^2)[b]	0.914	1.037	1.006	0.948
$\Delta\rho_{fin}$ (max / min), e $Å^{-3}$	0.75 / −0.56	0.71 / −0.61	0.73 / −0.43	0.36 / −0.36

[a] $R1 = \Sigma||F_o| - |F_c||/\Sigma|F_o|$, $wR2 = [\Sigma w(F_o^2 - F_c^2)^2/\Sigma w(F_o^2)^2]^{1/2}$, $w = [\sigma^2(F_o^2) + (AP)^2 + BP]^{-1}$, where $P = (\mathrm{Max}(F_o^2, 0) + 2F_c^2)/3$ and A and B are constants adjusted by the program; [b] $\mathrm{GoF} = S = [\Sigma w(F_o^2 - F_c^2)^2/(n_{obs} - n_{param})]^{1/2}$.

and aromatic ammoniums [1 – 8], for which interesting crystal structures and physical properties were expected. The ^{81}Br NQR frequencies at room and liquid N_2 temperatures of some zinc bromide complexes with pyridines have already been reported from the extensive investigations of complex compounds of MX_2 (M = Zn, Cd, Hg; X = Cl, Br, I) by Hiura [9]. Further, we report the crystal structures of the representative monoanionic and neutral complexes in the series of compounds presented in this paper in an attempt to clarify the origin of the stability of the crystalline states of the monoanionic complexes on the basis of information about the electronic charge distributions on the Br atoms.

Results and Discussion

Crystal structures of the monanionic and neutral complexes

The crystal structures of the monoanionic complexes (PyH)[$ZnBr_3$(Py)] (**1**) and (4-MePyH)-[$ZnBr_3$(4-MePy)] (**4**), and of the neutral complexes [$ZnBr_2$(4-MePy)$_2$] (**9**) and [$ZnBr_2(Py)_2$] (**10**), where Py and MePy stand for pyridine (C_5H_5N) and methyl-substituted pyridine ($CH_3C_5H_4N$), respectively, have been determined. The experimental conditions and crystallographic data are given in Table 1 [10]. The bond lengths and angles and other short contacts are listed in Table 2.

The crystals of **1** and **4** are triclinic with the space group $P\bar{1}$ and monoclinic with the space group $P2_1/c$, respectively. The monoanions are distorted tetrahedral in both structures; the averaged angles ∠Br–Zn–Br and ∠N–Zn–Br are 112.2° and 106.6° in [$ZnBr_3$(Py)]$^-$, and 111.8° and 107.0° in [$ZnBr_3$(4-MePy)]$^-$, respectively (Table 2). The angle relations show that a negligible difference is found in the geometry of the anions of the two compounds.

Fig. 1 shows a projection of the unit cell of **1** onto the *ac* plane. The asymmetric unit consists of a pair of PyH^+ and [$ZnBr_3$(Py)]$^-$ which are connected through a bifurcated hydrogen bond N(2)–H···Br(2) and ···Br(3). These units are stacked along [101], indicating the existence of π-π interactions between the pyridine rings [11]. Neighboring pyridine rings are separated by a distance of 3.96 Å between their

Table 2. Selected bond lengths (Å), bond angles (deg), and short intermolecular contacts (Å) in **1**, **4**, **9**, and **10**.

(PyH)[$ZnBr_3$(Py)] (**1**)[a]			
Zn–Br(1)	2.3712(6)	Br(1)–Zn–Br(2)	115.50(2)
Zn–Br(2)	2.3860(6)	Br(1)–Zn–Br(3)	112.67(2)
Zn–Br(3)	2.3982(6)	Br(2)–Zn–Br(3)	108.28(2)
Zn–N(1)	2.045(3)	N(1)–Zn–Br(1)	105.83(9)
		N(1)–Zn–Br(2)	106.08(9)
		N(1)–Zn–Br(3)	108.02(9)

[a] The bond angles deduced from the Zeeman effect measurements for three NQR lines of this compound are: $\angle Br(\nu_1)$–Zn–$Br(\nu_2)$ = 112.2°, $\angle Br(\nu_1)$–Zn–$Br(\nu_3)$ = 118.2°, $\angle Br(\nu_2)$–Zn–$Br(\nu_3)$ = 106.1° (ref. [9]).

(4-MePyH)[$ZnBr_3$(4-MePy)] (**4**)			
Zn–Br(1)	2.4011(6)	Br(1)–Zn–Br(2)	109.00(3)
Zn–Br(2)	2.3937(6)	Br(1)–Zn–Br(3)	113.53(2)
Zn–Br(3)	2.3813(6)	Br(2)–Zn–Br(3)	112.82(2)
Zn–N(1)	2.042(3)	N(1)–Zn–Br(1)	107.33(9)
		N(1)–Zn–Br(2)	108.86(9)
		N(1)–Zn–Br(3)	105.01(9)
$[ZnBr_2$(4-MePy)$_2]$ (**9**)			
Zn–Br(1)	2.3474(4)	Br(1)–Zn–Br(2)	105.65(6)
Zn–Br(2)	2.3555(4)	N(1)–Zn–Br(1)	109.76(6)
Zn–N(1)	2.040(2)	N(2)–Zn–Br(2)	105.65(6)
Zn–N(2)	2.061(2)	N(2)–Zn–Br(1)	108.32(6)
		N(1)–Zn–Br(2)	107.93(6)
		N(1)–Zn–N(2)	101.28(8)
$[ZnBr_2(Py)_2]$ (**10**)			
Zn–Br(1)	2.3494(5)	Br(1)–Zn–Br(2)	120.74(2)
Zn–Br(2)	2.3549(5)	N(1)–Zn–Br(1)	108.40(8)
Zn–N(1)	2.047(2)	N(2)–Zn–Br(2)	106.58(8)
Zn–N(2)	2.056(3)	N(2)–Zn–Br(1)	107.65(7)
		N(1)–Zn–Br(2)	107.37(8)
		N(1)–Zn–N(2)	105.07(10)

Short contacts in **1**

Connection	d(N···Br)	d(H···Br)	∠(N–H···Br)
N(2)$^{\#1}$–H···Br(2)	3.546(4)	2.90(3)	134(3)
N(2)$^{\#1}$–H···Br(3)	3.470(3)	2.78(3)	139(4)

$^{\#1}$ $1-x, 1-y, 1-z$.

Short contacts in **4**

Connection	d(N···Br)	d(H···Br)	∠(N–H···Br)
N(2)$^{\#2}$–H···Br(1)	3.324(4)	2.64(5)	140(4)

$^{\#2}$ $-x+1, -y, -z$.

Short contacts in **9**

Connection	d(C···Br)	d(H···Br)	∠(C–H···Br)
C(12)$^{\#2}$–H···Br(1)	3.754	2.849	154

$^{\#2}$ $-x, 1/2+y, 3/2-z$.

centroids, and their planes are tilted by an angle of 8.4°.

Fig. 2 shows the unit cell of **4** projected onto the *ac* plane. Both cationic 4-MePyH$^+$ and anionic [$ZnBr_3$(4-MePy)]$^-$ are piled up in columns along the *a* axis characterizing the structure. In the cationic columns, adjacent N(2)-pyridine rings are separated by a distance of 4.20 Å between their centroids, and their planes are tilted by an angle of 8.2°. In the anionic columns, the corresponding distance and angle for adjacent N(1)-pyridine rings are 4.00 Å and 2.9°, respectively. The components 4-MePyH$^+$ and [$ZnBr_3$(4-MePy)]$^-$ are bound together with a normal hydrogen bond of N(2)–H···Br(1). Further stabilization due to π-π interactions between the neighboring pyridine rings is also observed in the crystal structure of **4**.

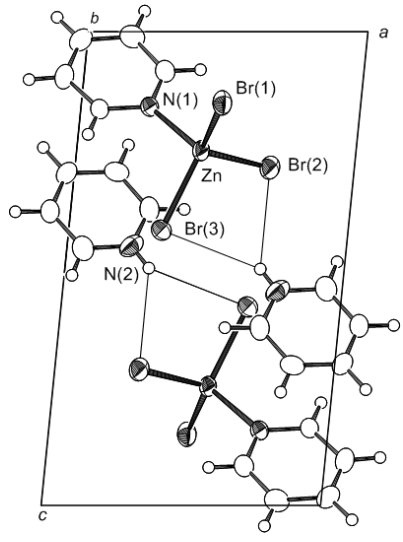

Fig. 1. The projection of the unit cell of (PyH)[$ZnBr_3$(Py)] (**1**) as seen along [010].

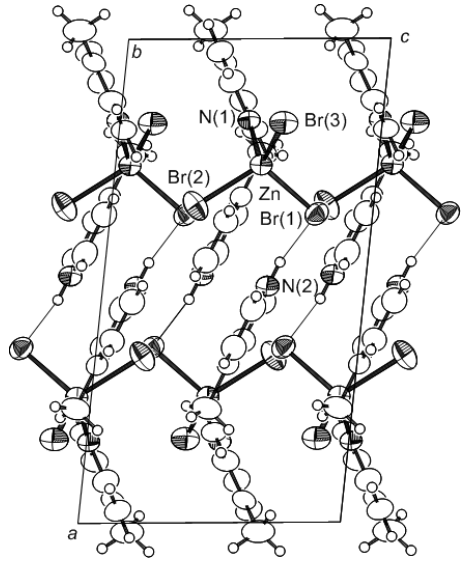

Fig. 2. The projection of the unit cell of (4-MePyH)[$ZnBr_3$(4-MePy)] (**4**) as seen along [010].

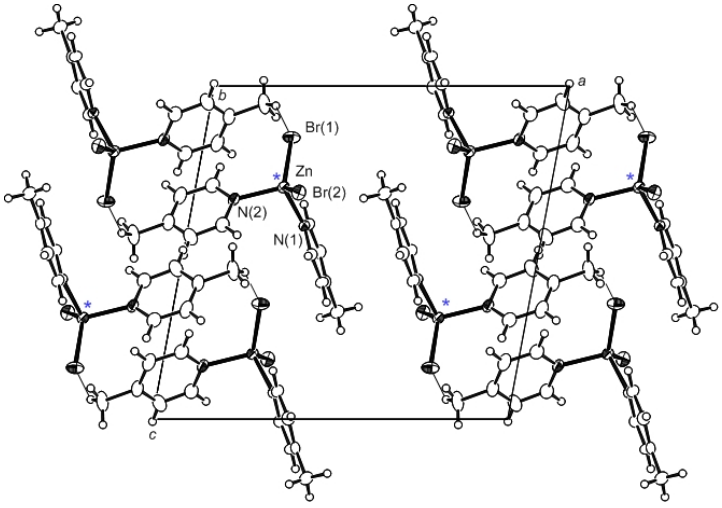

Fig. 3. The projection of the unit cell of [$ZnBr_2$(4-MePy)$_2$] (**9**) as seen along [010].

However, the pyridine rings are stacked up as parallel as possible in both **1** and **4**, but the replacement of Py by 4-MePy results in a quite different packing.

The crystal structures of both neutral complexes [$ZnBr_2$(4-MePy)$_2$] (**9**) and [$ZnBr_2$(Py)$_2$] (**10**) belong to the monoclinic system with the same space group $P2_1/c$ (Table 1). The structure of **9** has already been reported by Fanfani *et al.* [12], their structure being basically identical with the present structure. The structure of **10** is isomorphous to the structures of the chloride [13] and iodide [14] analogs. Figs. 3 and 4 show the projections on to the respective *ac* planes of the unit cells of **9** and **10**. The coordination around the Zn atoms is distorted tetrahedral in both structures: ∠Br–Zn–Br = 105.7°, ∠N–Zn–N = 101.3° and ∠N–Zn–Br = 107.9° (averaged) for **9**; ∠Br–Zn–Br = 120.7°, ∠N–Zn–N = 105.7° and ∠N–Zn–Br = 107.4° (averaged) for **10** (Table 2). Reflecting the slight bulkiness of 4-MePy compared to Py, the ∠N–Zn–N angle is larger in **10** than in **9**. The crystal structure of **9** consists of columns of stacked [$ZnBr_2$(4-MePy)$_2$] molecules, in which they are arrayed along [100], as illustrated by the molecules with asterisks in Fig. 3. In the columns the N(1)-pyridine rings of adjacent molecules face each other reversely parallel with a plane interval of 3.55 Å and a distance of 3.69 Å between the centroids of the rings. This situation may show the existence of π-π interactions between the pyridine rings of the paired molecules. In addition, the methyl group of the N(2)-pyridine ring points to the center of an adjacent N(1)-pyridine ring. The CH_3-π as well as the π-π interactions thus link the molecules

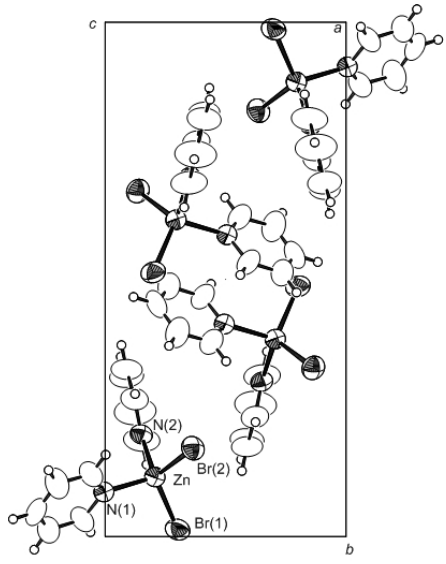

Fig. 4. The projection of the unit cell of [$ZnBr_2$(Py)$_2$] (**10**) as seen along [100].

to form the column structure along [100]. The planes of the N(2)-pyridine rings pile up infinitively along one direction in the *bc* plane reversing their faces alternatingly suggesting π-π interactions. The interval of parallel planes is 3.62 Å, and the distance between the centroids of two adjacent rings is 4.53 Å showing a reduced overlap compared with that of the N(1)-pyridine rings. In addition, there is a short contact Br(1)···H–C(methyl) of 2.85 Å which connects the columns.

In the crystal structure of **10** (Fig. 4), adjacent N(1)-pyridine rings are anti-parallel with a plane interval

Table 3. ^{81}Br NQR frequencies at 273 K for compounds **1** – **10**.

Compounds	ν (MHz)			
(PyH)[$ZnBr_3$(Py)] (**1**)	65.09	61.39	60.13	
	(64.908)[a]	(61.308)[a]	(60.058)[a]	
(2-MePyH)[$ZnBr_3$(2-MePy)] (**2**)	65.92	64.37	58.41	
(3-MePyH)[$ZnBr_3$(3-MePy)] (**3**)	66.65	63.58	57.77	
(4-MePyH)[$ZnBr_3$(4-MePy)] (**4**)	66.09	63.80	60.06	
	(60.830)[a]	(58.979)[a]	(57.049)[a]	
$(PyH)_2[ZnBr_4]$ (**5**)	63.15	60.36	59.99	57.72
	(62.750)[b]	(59.826)[b]	(59.826)[b]	(57.551)[b]
$(3\text{-MePyH})_2[ZnBr_4]$ (**6**)	61.16	57.04		
$(4\text{-MePyH})_2[ZnBr_4]$ (**7**)	65.57	59.97	58.08	55.97
$[ZnBr_2(2\text{-MePy})_2]$ (**8**)	70.90	67.31		
	(70.914)[a]	(67.463)[a]		
$[ZnBr_2(4\text{-MePy})_2]$ (**9**)	68.99	68.58		
	(68.703)[a]	(68.297)[a]		
$[ZnBr_2(Py)_2]$ (**10**)	(69.723)[a]	(67.800)[a]		

[a] The values at 296 K in ref. [9] in parentheses; [b] the values at r. t. in ref. [5] in parentheses.

of 3.77 Å and a distance of 3.86 Å between the centers of adjacent rings, suggesting weaker π-π interactions than in **9**. On the other hand, though the N(2)-pyridine rings are piled up infinitely in the *c* direction with their planes almost parallel to the *a* axis, adjacent N(2)-pyridine rings are inclined by 25.4° to each other, indicating poor interactions. It is noticed throughout **1**, **4**, **9**, and **10** that (1) the pyridine rings are oriented as parallel as possible to enable π-π overlap, and (2) the 4-CH_3 substituent enhances the π-π interactions between the pyridine rings probably owing to its electron releasing ability.

Hiura [9] has reported that the frequencies of the two ^{79}Br NQR resonance lines of **10** show a strange temperature dependence. The lower frequency line shows a positive dependence with a rather large temperature coefficient around r. t. where the curve has a reflection point. The other line has a negative temperature coefficient but has also a reflection point around r. t. He has suggested that this phenomenon may have its origin in the intermolecular bonds in which the Br atoms and the pyridine ring H atoms are involved. However, such short contacts were not observed in the present structural study. We therefore inquired about the origin of these changes which may be due to the torsion angle Br–Zn–pyridine ring and/or to the packing in the structure.

^{81}Br NQR frequencies of the complexes of $ZnBr_2$ with pyridines

The temperature dependence of the ^{81}Br NQR frequencies of (PyH)[$ZnBr_3$(Py)] (**1**) and (*n*-MePyH)[$ZnBr_3$(*n*-MePy)] (*n* = 2 (**2**), 3 (**3**), 4 (**4**)) measured between 77 and *ca.* 320 K are shown in Fig. 5, and the frequency values at 273 K are listed in Table 3. Three

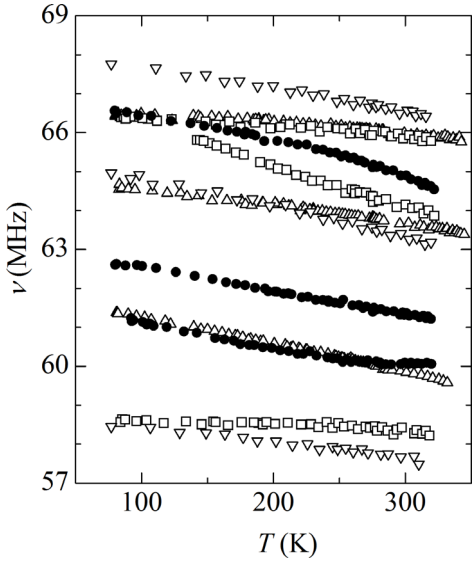

Fig. 5. The temperature dependence of the ^{81}Br NQR frequencies of (PyH)[$ZnBr_3$(Py)] (**1**): •, (2-MePyH)[$ZnBr_3$(2-MePy)] (**2**): □, (3-MePyH)[$ZnBr_3$(3-MePy)] (**3**): ▽, and (4-MePyH)[$ZnBr_3$(4-MePy)] (**4**): △.

NQR lines of **1** with the signal intensity ratio of 1 : 1 : 1, denoted as ν_1 to ν_3 in decreasing frequency order, are consistent with the number of nonequivalent Br atoms in the crystal structure. All the resonance frequencies decrease continuously with temperature, without showing any sign of phase transitions. The average frequency of the closely situated ν_2 and ν_3 is lower by *ca.* 4 MHz than the frequency of ν_1. In addition, both lines exhibit a slight but unusual upward curvature in the higher temperature regions. These features of frequency lowering and upward curvature may be explained by a weakening of the N–H···Br hydrogen bonds with increasing temperature [15], because both

Br(2) and Br(3) atoms participate in the bifurcated hydrogen bonding. The ∠Br–Zn–Br angles of the anions in **1** have previously been deduced from measurements of the Zeeman effect on the NQR lines [9] to be 112.2, 118.2, and 106.1° for Br(ν_1)–Zn–Br(ν_2), Br(ν_1)–Zn–Br(ν_3), and Br(ν_2)–Zn–Br(ν_3), respectively. The comparison of these values with the present X-ray results allow us to assign ν_1, ν_2, and ν_3 to the Br(1), Br(3), Br(2) atoms, respectively, with only small differences between the corresponding values.

All three compounds of (*n*-MePyH) [$ZnBr_3$(*n*-MePy)] (*n* = 2 (**2**), 3 (**3**), 4 (**4**)) gave three NQR lines with an intensity ratio of 1 : 1 : 1 throughout the observed temperature range. The continuous change of the frequencies with temperature shows no sign of phase transitions in these compounds within the observed temperature range (Fig. 5). Though the crystal structures of **2** and **3** have not yet been determined, the existence of [$ZnBr_3$(*n*-MePy)]$^-$ ions in their crystals is obvious, because the averaged ^{81}Br NQR frequencies $\langle\nu\rangle$ are almost constant throughout the series of the compounds with the values of **1**: 62.20, **2**: 62.90, **3**: 62.67, and **4**: 63.32 MHz at 273 K. All spectra of the *n*-MePy complexes consist of one low- and two high-frequency lines separated significantly, though the tendency in **4** is less pronounced compared to the others. This may be an indication of the similarity of their structures. The two lower frequency lines ν_2 and ν_3 of **1** are assigned to the Br(3) and Br(2) atoms, respectively, which participate in the bifurcated hydrogen bond (Fig. 1) as mentioned above. On the other hand, the Br(1) atom in **4** is the only one atom which participates in a hydrogen bond, *viz.* N(2)–H···Br(1). Then it seems appropriate to assign the lowest line of **4** to Br(1). The lowest NQR resonance lines of **2** and **3** may then be assigned to the Br atoms of which N–H···Br hydrogen bonding is expected from their NQR spectra. At this time, the strength of N–H···Br hydrogen bonds in the series of **1**, **2**, **3**, and **4** may be judged from the frequency differences between that of the lowest line and the averaged frequencies $\langle\nu\rangle$ in each compound, because it is usually observed that for stronger intermolecular hydrogen bonds the frequencies of the atoms concerned are lower. This criterion gives the following order of the strength of hydrogen bonding: (3-MePyH)[$ZnBr_3$(3-MePy)] > (2-MePyH)[$ZnBr_3$-(2-MePy)] > (4-MePyH)[$ZnBr_3$(4-MePy)] > (PyH)[$ZnBr_3$(Py)] (the averaged frequency was used for the bifurcated hydrogen bond in the last compound). This order is supported by the substituent effects: (1) the increased electron releasing ability of Me compared to H, and (2) the lower donor ability of 2-Me compared to 3-Me due to an *ortho* effect.

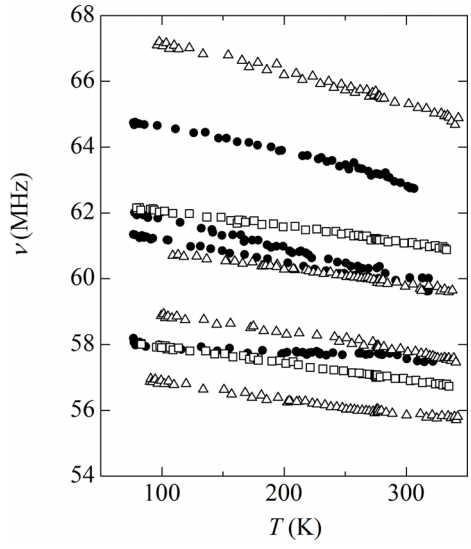

Fig. 6. The temperature dependence of the ^{81}Br NQR frequencies of $(C_5H_5NH)_2[ZnBr_4]$ (**5**): •, (3-MePyH)$_2$[$ZnBr_4$] (**6**): □, and (4-MePyH)$_2$[$ZnBr_4$] (**7**): △.

The temperature dependence of the ^{81}Br NQR frequencies of $(PyH)_2[ZnBr_4]$ (**5**) and (*n*-MePyH)$_2$-[$ZnBr_4$] (*n* = 3 (**6**), 4 (**7**)) observed between 77 K and around r. t. is shown in Fig. 6. No NQR line was observed for (2-MePyH)$_2$[$ZnBr_4$] in spite of the search at several different temperatures.

All the observed resonance lines for **5**, **6**, and **7** exhibited the normal negative temperature dependence without showing any sign of phase transitions. We have already reported the temperature dependence of the ^{81}Br NQR frequencies of **5** [5]. There are some deviations between the values in ref. [9] and ours (Table 3). In the drying process of the crystals of **5**, the hydrated compounds $(PyH)_2[ZnBr_4]\cdot nH_2O$ were obtained depending on the drying agents. The NQR results of these hydrates will be reported elsewhere [16]. With the same intensity, two and four ^{81}Br NQR lines were observed for **6** and **7**, respectively. Though the crystal structures of these compounds have not yet been determined, tetrahedral $ZnBr_4^{2-}$ ions are expected to exist in these crystals, since the averaged resonance frequencies of each compound at 273 K are *ca.* 60 MHz, with individual values of 60.31, 59.27, and 59.90 MHz for **5**, **6**, and **7**, respectively. The numbers of NQR lines further indicate that distorted tetrahedral $ZnBr_4^{2-}$ ions with four non-equivalent Br atoms exist in the crystals

of **5** and **7**, but a more symmetrical tetrahedral $ZnBr_4^{2-}$ ion exists on a symmetry plane and/or a 2-fold axis in the structure of **6**. It is noticed that the ^{81}Br NQR spectra are widely spread in frequency (Fig. 6), showing the existence of N–H···Br hydrogen bonds between cations and anions which can be different from compound to compound.

The temperature dependence of the ^{81}Br NQR resonance frequencies in $[ZnBr_2(n\text{-MePy})_2]$ (n = 2 (**8**), 4 (**9**)) is shown in Fig. 7. Two lines for each compound exhibit normal frequency *vs.* temperature curves without showing any sign of phase transitions between 77 K and r. t. The frequencies have already been reported for both compounds at several temperatures [9], in good agreement with the present results. The averaged ^{81}Br NQR frequencies in $[ZnBr_2(Py)_2]$ and $[ZnBr_2(n\text{-MePy})_2]$ are 68.76 and 68.94 MHz at 273 K, respectively, and thus higher than those in the related ionic compounds, confirming that these compounds form molecular crystals. The frequency ranges of the ^{81}Br NQR lines of these compounds are narrow, almost half of those of the related ionic compounds. This is consistent with the smaller crystal field effect in the molecular crystals and also with the absence of the N–H···Br hydrogen bonds in these crystals.

Zn-Br chemical bonding in the complexes of $ZnBr_2$ with pyridines

It seems interesting to compare the nature of the Zn–Br bonds in the monoanionic complexes to those of the dianionic and the neutral complexes, because the occurrence of the redistribution reactions may indicate that the crystalline states of monoanionic complexes are more stable than those of the corresponding dianionic and neutral complexes. We carried out *ab initio* MO calculations for the series of complex compounds by using WINGAMESS with a 6-31G* basis set [17]. The results of the calculations predict the optimized geometrical structure of the $[ZnBr_3(Py)]^-$ ion to be of C_s symmetry with one Br(I) atom on a mirror plane and two Br(II) atoms related by this plane, which is a higher symmetry than that observed in the crystal structure. The structure of the $[ZnBr_3(4\text{-MePy})]^-$ ion was calculated to be of C_1 symmetry which is consistent with the crystal structure. The calculated bond lengths and bond angles are as follows: Zn–Br(I) = 2.446, Zn–Br(II) = 2.452 Å, ∠Br(I)–Zn–Br(II) = 115.9 and ∠Br(II)–Zn–Br(II′) = 117.5° for the $[ZnBr_3(Py)]^-$ ion; averaged Zn–Br = 2.452 Å and averaged ∠Br–Zn–Br = 116.4° for the $[ZnBr_3(4\text{-MePy})]^-$ ion. The calculated bond lengths and angles in both compounds are slightly larger than those of the X-ray data (Table 2), showing the contraction of the $ZnBr_3$ moieties in the crystal. The net charges ρ^* on the Br atoms were calculated according to the Mulliken population analysis [14] to be −0.699 e and −0.713 e for Br(I) and Br(II) in the $[ZnBr_3(Py)]^-$ ion, respectively, and −0.710 e on average for Br in the $[ZnBr_3(4\text{-MePy})]^-$ ion. The average values of the net charges $\langle|\rho^*|\rangle$/e on the Br atoms are listed in Table 4.

Table 4. The averaged unbalanced p electron numbers U_p and the averaged net charges $\langle\rho\rangle$ and $\langle|\rho^*|\rangle$/e for the Br atoms in compounds **1** – **10**.

Compounds	U_p	$\langle\rho\rangle$	$\langle\|\rho^*\|\rangle$/e[a]
(PyH)[$ZnBr_3$(Py)] (**1**)	0.193	0.768	0.709
(2-MePyH)[$ZnBr_3$(2-MePy)] (**2**)	0.196	0.770	0.709
(3-MePyH)[$ZnBr_3$(3-MePy)] (**3**)	0.195	0.771	0.709
(4-MePyH)[$ZnBr_3$(4-MePy)] (**4**)	0.197	0.768	0.710
$(PyH)_2[ZnBr_4]$ (**5**)	0.188	0.779	0.772
$(3\text{-MePyH})_2[ZnBr_4]$ (**6**)	0.184	0.784	0.772
$(4\text{-MePyH})_2[ZnBr_4]$ (**7**)	0.186	0.781	0.772
$[ZnBr_2(2\text{-MePy})_2]$ (**8**)	0.215	0.747	0.653
$[ZnBr_2(4\text{-MePy})_2]$ (**9**)	0.214	0.748	0.664
$[ZnBr_2(Py)_2]$ (**10**)	0.214	0.748	0.659

[a] The averaged values of ρ^* are calculated with WINGAMESS [14].

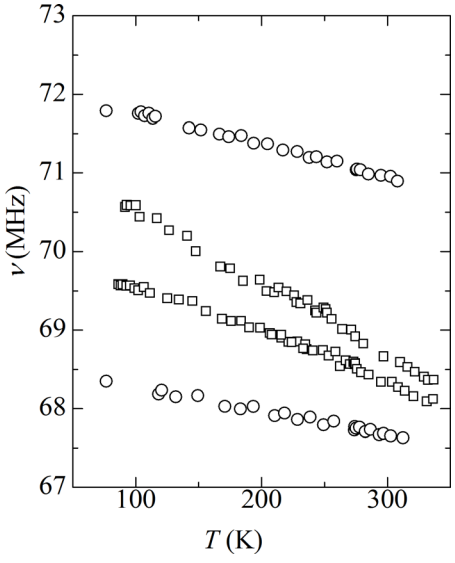

Fig. 7. The temperature dependence of the ^{81}Br NQR frequencies of $[ZnBr_2(2\text{-MePy})_2]$ (**8**): ○ and $[ZnBr_2(4\text{-MePy})_2]$ (**9**): □.

Conversely, the net charges ρ were also calculated from the NQR parameters by the Townes-Daily analysis [18]. In this analysis the valence electron populations of Br atoms were taken as $1+\rho$ for the $4p_\sigma$ bonding orbital with s hybridization and as 2 for the

respective three lone pair orbitals, *i. e.* an antibonding orbital and the $4p_x$ and $4p_y$ nonbonding orbitals. In this case, the atomic orbital populations of the Br atoms are $N_z = (1-\rho)(1-s^2)+2s^2$, $N_x = 2$, and $N_y = 2$, where N_z, N_x, and N_y denote the populations in $4p_z$, $4p_x$, and $4p_y$, respectively, and s^2 denotes the degree of s hybridization. Then, the number of unbalanced p electrons, U_p, is obtained by

$$U_p = |N_z - (N_x + N_y)/2| = (1-\rho)(1-s^2) \quad (1)$$

U_p is expressed as

$$U_p = |(e^2Qq/h)_{obs}/(e^2Qq/h)_{atom}|, \quad (2)$$

where $(e^2Qq/h)_{obs}$ is the observed quadrupole coupling constant and $(e^2Qq/h)_{atom}$ is the atomic quadrupole coupling constant of 643.032 MHz for the ^{81}Br atom. According to the usual manner in which the axially symmetrical electric field gradients are applied for the terminal Br atoms, we arrive at $(e^2Qq/h)_{obs} = 2\nu$. Further, we set s^2 = 0.15 for atoms with a difference in electronegativity exceeding 0.25 units for two bonded atoms as postulated in the original paper of Townes and Dailey [18]. Now, the ρ values corresponding to the net charges on the atoms are obtained from the ^{81}Br NQR frequencies. The averaged values of the net charges $\langle\rho\rangle$ are listed in Table 4.

Considering the assumptions made in both methods a good correlation seems to be seen between the average net charges on the Br atoms $\langle\rho\rangle$ and $\langle|\rho^*|\rangle$/e (Table 4). A decreasing order in the net charges on the Br atoms in each group $ZnBr_4^{2-}$ (**5**, **6**, **7**) > $ZnBr_3(R)^-$ (**1**, **2**, **3**, **4**) > $ZnBr_2(R)_2$ (**8**, **9**) is apparent, as the negative ionic charge on the relevant moieties decreases from −2 to 0. It is noticed that the agreement between $\langle\rho\rangle$ and $\langle|\rho^*|\rangle$/e is fairly good for the $ZnBr_4^{2-}$ complexes, and that the discrepancies increase from monoanions to neutral complexes. The values of $\langle\rho\rangle$ are less dependent on the types of complex compounds than $\langle|\rho^*|\rangle$/e. Going from the $ZnBr_4^{2-}$ complexes to the neutral complexes, the variations of $\langle\rho\rangle$ are almost one third of those of $\langle|\rho^*|\rangle$/e. The differences between $\langle\rho\rangle$ and $\langle|\rho^*|\rangle$/e appear to originate mainly from the crystal field effect, since only the molecular parts are taken for the calculation of $\langle|\rho^*|\rangle$/e. This means that the differences (*i. e.*, the apparent increase of the polarization in the Zn–Br bonds) are the largest for the neutral complexes $ZnBr_2(R)_2$, smaller for the $ZnBr_3(R)^-$ anions and negligible for the $ZnBr_4^{2-}$ complexes when the isolated chemical units are brought into the crystalline states. The larger polarization of Zn–Br for the neutral complexes may be induced by the π interactions between the pyridine rings. The differences between the monoanionic and dianionic complexes, for which the crystals are ionic in nature, may be explained by the same effect.

In conclusion, the comparison of intermolecular interactions existing in the crystals of a series of different compounds indicates that the dominant stability of monoanionic complexes may be attributed mainly to two distinctive interactions: (1) the π-π and where applicable CH_3-π interactions between the pyridine rings, and (2) the electrostatic interactions between cations and anions including the N–H···Br hydrogen bonds which are weaker or negligible for neutral complexes.

Table 5. Elemental analyses of C, H, and N: found % (calcd. %).

Compounds	C	H	N
1	26.01 (25.86)	2.38 (2.38)	6.09 (6.03)
2	28.62 (29.27)	3.03 (3.07)	5.55 (5.68)
3	29.21 (29.27)	3.02 (3.07)	5.66 (5.68)
4	29.38 (29.27)	3.07 (3.07)	5.70 (5.68)
5	21.72 (21.32)	2.32 (2.50)	5.07 (4.97)
6	24.34 (25.14)	2.68 (2.81)	4.74 (4.88)
7		too hygroscopic	
8	35.10 (35.02)	3.43 (3.42)	6.75 (6.80)
9	35.00 (35.02)	3.41 (3.42)	6.81 (6.80)

Experimental Section

(PyH)$_2$[ZnBr$_4$](**5**) and *(n-MePyH)$_2$[ZnBr$_4$]*(n = 3 (**6**), 4 (**7**)) were prepared from dilute hydrobromic acid solutions of a mixture of the pyridine and $ZnBr_2$ with a molar ratio of 2 : 1. The colorless tabular crystals obtained were dried over P_2O_5 in desiccators.

[ZnBr$_2$(Py)$_2$](**10**) and *[ZnBr$_2$(n-MePy)$_2$]*(n = 2 (**8**), 4 (**9**)) were prepared according to the published procedure [9] by mixing pyridine and $ZnBr_2$ in 99.5 % ethanol with a molar ratio of 2 : 1. After mixing, colorless powders appeared immediately. Colorless feather-like crystals were recovered through recrystallization from 99.5 % ethanol.

(PyH)[ZnBr$_3$(Py)] (**1**) and *(n-MePyH)[ZnBr$_3$(n-MePy)]* (n = 2 (**2**), 3 (**3**), 4 (**4**)) were prepared by dropwise addition of an ethanol solution of [$ZnBr_2(Py)_2$] or [$ZnBr_2$(*n*-$MePy)_2$] to an ethanol solution of $(PyH)_2[ZnBr_4]$ or (*n*-$MePyH)_2[ZnBr_4]$ under reflux. The results of chemical analyses are shown in Table 5. Needle-shaped crystals of **1** and prismatic ones of **4** suitable for X-ray measurements were prepared from the 99.5 % ethanol solutions by slow evaporation of the solvent. For elemental analyses see Table 5.

Crystal structure determinations

The structures of **1**, **4**, **9**, and **10** were determined using a four-circle X-ray diffractometer Oxford Diffraction Xcalibur with Sappire CCD Detector. (MoK_α radiation, λ = 0.71073 Å, graphite monochromator). All calculations were performed using SHELX-97 [19]. The crystal structures of **1** and **9** were determined at 150 K, since they were found to be disordered at ambient temperature. On the other hand, the NQR spectra of these compounds could be observed without any indications of disorder around r. t.

NQR spectra

The ^{81}Br nuclear quadrupole resonance (NQR) spectra were observed by using a home-made super-regenerative-type oscillator at temperatures above 77 K. The resonance frequencies were determined by a counting method. The accuracy of the frequency measurements is estimated to be within $\pm$0.05 MHz.

[1] K. Horiuchi, H. Ishihara, H. Terao, *J. Phys. Condens. Matter* **2000**, *12*, 4799 – 4806.

[2] P. Sondergeld, H. Fuess, H. Ishihara, S. A. Mason, W. W. Schmahl, *Z. Naturforsch*. **2000**, *55a*, 801 – 809.

[3] P. Sondergeld, H. Fuess, H. Ishihara, W. W. Schmahl, *Z. Kristallogr.* **2001**, *216*, 462 – 468.

[4] H. Ishihara, N. Hatano, K. Horiuchi, H. Terao, *Z. Naturforsch.* **2002**, *57a*, 343 – 347.

[5] K. Horiuchi, H. Ishihara, N. Hatano, S. Okamoto, T. Gushiken, *Z. Naturforsch*. **2002**, *57a*, 425 – 430.

[6] K. Horiuch, H. Ishihara, *Hyperfine Interact.* **2004**, *159*, 149 – 155.

[7] Y. Furukawa, H. Terao, H. Ishihara, T. M. Gesing, J.-C. Buhl, *Hyperfine Interact.* **2004**, *159*, 143 – 148.

[8] N. Hatano, M. Nakashima, K. Horiuchi, H. Terao, H. Ishihara, *Z. Naturfosch.* **2008**, *63b*, 1181 – 1186.

[9] M. Hiura, *J. Sci. Hiroshima Univ.* **1982**, *A45*, 383 – 405.

[10] CCDC 731727 (**1**), 731728 (**4**), 785987(**9**), and 785988(**10**) contain the supplementary crystallographic data for this paper. These data can be obtained from The Cambridge Crystallographic Data Centre *via* www.ccdc.cam.ac.uk/data_request/cif.

[11] H. Takaynagi, Y. Toubai, M. Goto, S. Yamaguchi, H. Ogura, *Chem. Pharm. Bull.* **1991**, *39*, 2491 – 2493.

[12] L. Fanfani, A. Nunzi, P. F. Zanazzi, *Acta Crystallogr*. **1972**, *B28*, 323 – 325.

[13] W. L. Steffen, G. J. Palenik, *Acta Crystallogr*. **1976**, *B32*, 298 – 300.

[14] J. F. Le Querler, M. M. Borel, A. Leclaire, *Acta Crystallogr*. **1977**, *B33*, 2299 – 300.

[15] H. Bayer, *Z. Physik*, **1951**, *130*, 227 – 238; D. Nakamura, T. Ikeda, M. Kubo, *Coord. Chem. Rev.* **1975**, *17*, 281 – 316.

[16] H. Ishihara, N. Hatano, K. Horiuchi, H. Terao, I. Svoboda, H. Fuess, to be submitted.

[17] Calculations were done with using WINMOSTAR (http://winmostar.com/index_en.html) and calculations with a 6-31G* basis set for optimized structures of $[ZnBr_3(C_5H_5N)]^-$, $[ZnBr_3(n\text{-}CH_3C_5H_4N)]^-$ (n = 2, 3, 4), $[ZnBr_4]^{2-}$, and $[ZnBr_2(n\text{-}CH_3C_5H_4N)_2]$ (n = 2, 4) by using WINGAMESS, GAMESS (version 11) obtainable from http://www.msg.chem.iastate.edu /gamess/download.html. See also: M. W. Schmidt, K. K. Baldridge, J. A. Boatz, S. T. Elbert, M. S. Gordon, J. H. Jensen, S. Koseki, N. Matsunaga, K. A. Nguyen, S. J. Su, T. L. Windus, M. Dupuis, J. A. Montgomery, *J. Comput. Chem.* **1993**, *14*, 1347 – 1363.

[18] E. A. C. Lucken, *Nuclear Quadrupole Coupling Constants*, Academic Press, New York, **1969**, pp. 120 – 146; C. H. Townes, B. P. Dailey, *J. Chem. Phys*. **1949**, *17*, 782 – 796.

[19] G. M. Sheldrick, SHELXS/L-97, Programs for Crystal Structure Determination, University of Göttingen, Göttingen (Germany) **1997**. See also: G. M. Sheldrick, *Acta Crystallogr.* **1990**, *A46*, 467 – 473; *ibid.* **2008**, *A64*, 112 – 122.